TRANSVERSE DAMPER AND STABILITY DIAGRAM

S. A. Antipov[1*], D. Amorim[2], N. Biancacci, X. Buffat, E. Métral, N. Mounet, A. Oeftiger[3], D. Valuch
CERN, Geneva, Switzerland, [1] also at DESY, Hamburg, Germany,
[2] also at Synchrotron SOLEIL, Gif-sur-Yvette, France, [3] also at GSI, Darmstadt, Germany

Abstract

We describe a proof-of-principle test to measure Landau damping in a hadron ring using a destabilizing transverse feedback acting as a controllable source of beam coupling impedance. The test was performed at the Large Hadron Collider and stability diagrams for a range of its Landau octupole strengths have been measured for its injection energy of 450 GeV. In the future, the procedure could become an accurate way of measuring stability diagrams throughout the machine cycle.

LANDAU DAMPING

A common technique of measuring Landau Damping is by means of Beam Transfer Function (BTF) measurements [1], where the frequency dependence of the response to forced beam oscillations is used to quantify the Stability Diagram (SD) [2]. BTF has been successfully used to measure SDs at GSI [3], RHIC [4] and at injection energy in LHC [6, 7]. The method has some limitations though: first, it might be challenging to maintain both good beam stability and high signal to noise ratio when driving the oscillation as seen at top energy in LHC [7]. Second and most importantly, the measurement does not test the strength of the Landau damping itself, but the transfer function. Numerous approximations are usually made to obtain the SD from the BTF: the synchrotron frequency spread is neglected, the betatron frequency spread is assumed to be small, the beam response to an external excitation is assumed to be linear.

A new alternative approach for measuring the strength of Landau damping involves using the transverse feedback with a reverted polarity (anti-damper) to excite a collective mode in the beam. The anti-damper such acts as a controllable source of beam coupling impedance. By knowing the strength of the feedback excitation, and observing at which feedback gain the beam becomes unstable, one obtains a direct measurement of the strength of Landau damping in the synchrotron. Further, with an accurate control over the feedback phase one can explore the full complex plane of tune shift and growth rate. One can such derive the SD and compare with theoretical predictions. In this paper we describe the first proof of principle test to measure the strength of Landau damping created by the LHC octupole system at 450 GeV injection energy.

* Sergey.Antipov@desy.de

MEASUREMENT OF LANDAU DAMPING AT LHC

Feedback as Controlled Impedance

If the variation of the feedback's dynamic response over the bunch length can be neglected, i.e. it is 'flat', it can be described as a constant wake force acting on the beam $W(z) = W_0 = const$. This is true e.g. for the LHC transverse feedback whose bandwidth goes up to 40 MHz or 1/10 of the radio frequency (RF) period or RF bucket width. This wake function corresponds to a δ-function-like coupling impedance (see [8] or [9] for reference):

$$Z_d(\omega) \sim ig \times e^{i\phi} \times \delta(\omega), \qquad (1)$$

where g stands for feedback gain in inverse turns and ϕ for its phase: 0 indicates a resistive feedback (picking up on beam position) and 90 deg a reactive one (picking up on transverse beam momentum). A resistive feedback thus drives a coherent beam mode upwards in the diagram, driving it unstable, with an instability growth rate of $-g$ (Fig. 1). Such a system has been proposed for the IOTA ring [10, 11], where the researchers considered an anti-damper with $\phi = 0$.

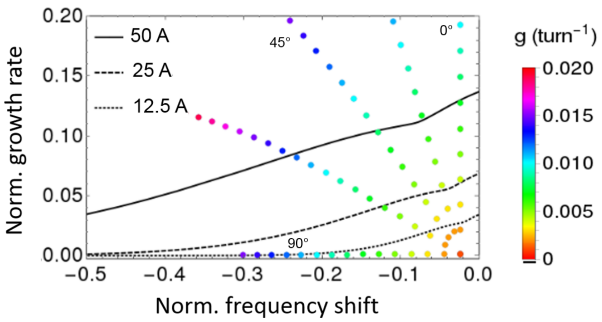

Figure 1: Controlling the gain and the phase of the feedback one explores the full relevant area of SD in LHC. Real and imaginary mode frequency shifts are normalized by the synchrotron frequency ω_s. SDs for a nominal 1.0 μm emittance Gaussian beam distribution are shown in black for various Landau octupole currents.

A realistic impedance of various accelerator components ranges from inductive impedance of high-Q RF modes, to broadband imaginary impedance of bellows and tapers. These impedances can be modelled by different phases of the feedback: from 0 for a purely imaginary tune shift to 90 deg for a purely real one. In practice, a variation of the phase is convenient to achieve with two feedback pick-ups: one picking up on the beam momentum and the other on its position. The LHC transverse feedback system features

two pick-ups (Fig. 2). This allows producing an arbitrary complex gain $g \times e^{i\phi}$ by adjusting phase delay between them and their gain [12].

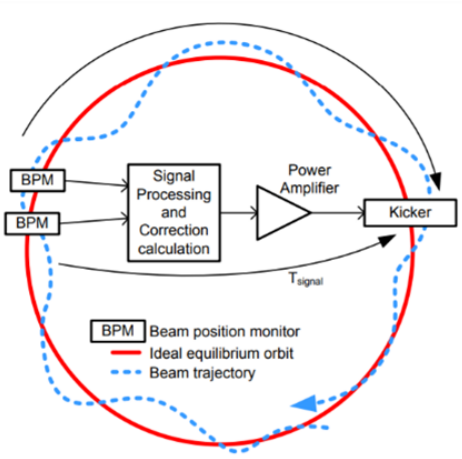

Figure 2: LHC feedback system uses two pickups per plane allowing acting independently on both beam transverse position and its transverse momentum.

It has to be noted that in normal operation the LHC transverse feedback phase setting is optimized for a particular tune value. When operating away from the optimal tune, the phase of the pickup signal receives an error with respect to an ideal value. The error is deterministic and occurs merely from the specifics of signal processing. The error vanishes for phase shifts of 0 and $\pi/2$, and is largest for $\pi/4$. For the MD parameters with the tune close to 0.27 the error should have never exceeded 4 deg (Fig. 3). Furthermore, the impact of the pickup phase error on the transverse damper phase seen by the beam is actually smaller, since the damper sums signals from two pickups, each with a different relative phase to the kicker. Our estimates suggest that the phase error seen by the beam is sufficiently small and should not exceed 1 deg at the nominal LHC tune settings.

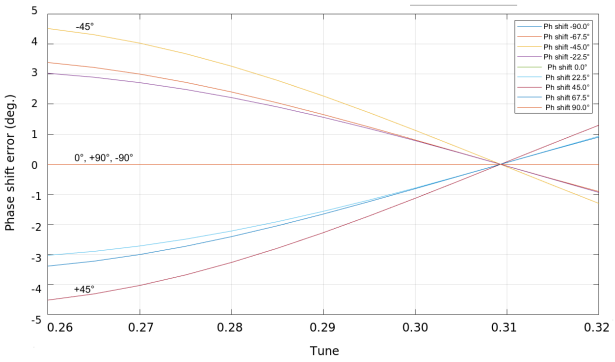

Figure 3: Signal processing phase error as a function of tune (horizontal axis) and the requested phase shift (colored traces) in a range from -90 to +90 degrees.

Choice of parameters

In order to have a good comparison with theory it is beneficial to perform a measurement at the nominal settings at the top energy of 6.5 TeV, where the optics is well under control, space charge is negligible, and there are plenty of experimental data for instability thresholds and the impedance to compare with. Such a measurement however requires a lot of machine time to perform, which is detrimental for obtaining reproducible results. On the other hand, performing a measurement at the injection energy of 450 GeV allows for a rapid machine setup and re-injection to perform multiple repetitive measurements; also working at injection energy allows applying a large octupolar detuning in order to stabilize the beam without the need of resorting to the feedback, which simplifies the measurement procedure. The space charge tune shift remains small when using the low intensity pilot beams, while the low beam intensity also minimizes mode tune shift from beam coupling impedance.

Having a single dominating coherent mode is useful for being able to draw accurate predictions on the instability growth rate at various settings of feedback gain and phase. For example, at a nominal beam intensity and relatively high chromaticity there may be several azimuthal modes with similar growth rates. Which of them becomes unstable first in the measurement is then determined by the shape of the SD and the mode frequency shift from impedance (Fig. 4). While, in principle, these effects can be simulated (e.g. by using a Vlasov solver) they also add unnecessary parameters to the measurement procedure, which might be not very well known or poorly controlled. Therefore such interference of different modes should be avoided when designing the experiment to measure Landau damping.

Based on the above considerations and limited by the time constraint of a realistic LHC machine study we have chosen to work at nominal LHC injection settings with an injection pilot beam, i.e. a single bunch of 0.5×10^{10} p with 1 μm normalized rms emittance. At these parameters the azimuthal dipolar head-tail mode typically dominates the landscape with higher order modes featuring much weaker growth rates. Beam and machine parameters are summarized in Table 1.

In LHC the betatron frequency spread required to produce the Landau damping is largely generated by a dedicated system of 84 focusing and 84 defocusing 30 cm long superconducting octupoles [14]. The initial calibration measurement was performed with the betatron tune spread provided only by the machine nonlinearities. This measurement is needed to confirm the experimental procedure and quantify the action of the feedback as the source of controlled impedance. Then another set of measurements was performed with Landau damping produced by several configurations of relatively high Landau octupole currents: ±11 and +17 A, which correspond to roughly 4 and 7×10^{-5} rms tune spread. This measurement was repeated at about nominal ring chromaticity of $Q' = +14$ and at low chromaticity of $Q' = +3$.

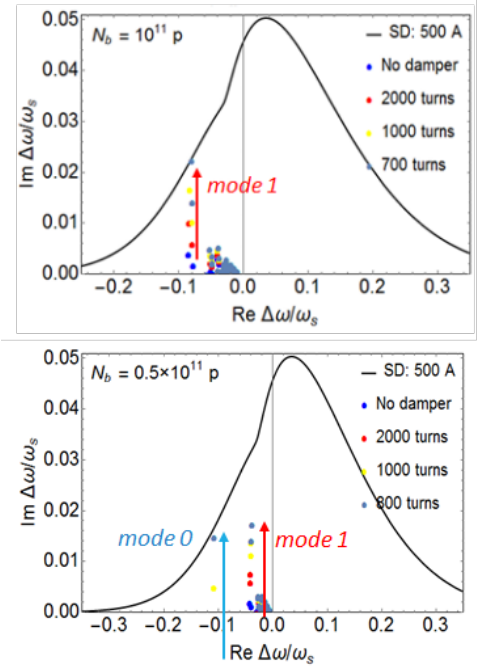

Figure 4: At Top energy and Nominal machine settings there could be several interfering modes with similar growth rates, depending on beam intensity. Top – nominal intensity of 10^{11} ppb, bottom – half the beam intensity. E = 6.5 TeV, Q' = 15, I_{oct} = +500 A, ϵ_n = 2.5 μm, nominal collimator settings.

Feedback calibration

In order to ensure an independent control over both the feedback gain and phase, the system was calibrated with no octupole current at three anti-damper phases: 0, 45 and 67.5 deg. At each phase the feedback excited a beam instability and the growth rate of the center-of-mass oscillations was measured as a function of the feedback gain. An example of raw data is shown in Fig. 5 and a larger data set is provided in the Appendix.

Table 1: Key parameters used for the study

Parameter	**Value**
Beam energy	450 GeV
Beam intensity	0.5×10^{10} ppb
Number of bunches	1
Norm. tr. emittance, rms	1.0 – 1.1 μm
Bunch length, $4\sigma_{rms}$	1 ns
Coupling, $\lvert C^- \rvert$	0.001
RF voltage	6 MV
Tunes: x, y, z	0.275, 0.295, 0.005
Chromaticity, Q'	14
Synch. freq., ω_s	0.03 rad^{-1}
SC tune shift	$O(10^{-4})$

An instability has been declared if the beam centroid excursion from the reference orbit exceeded 200 μm, which corresponds to the order of an rms beam size at the pickup locations. After triggering the instability, the last 64'000 turns of beam position data were saved for future processing. In order to assess the instability growth rate from the data x_i, it has been first passed through a low-pass digital filter to subtract any constant offset $y_i = x_{i+1} - x_i$. Then the oscillation envelope was obtained with a 50-turn moving Gaussian filter applied to y^2. Finally, a linear interpolation with a 5000-turn moving window was applied to $\log y^2$ and the growth rate was determined as $1/2$ the maximum slope.

Examining the data we realised that the measurements done at the smallest gains probably had the beam emittance spoiled due to the approach we took – slowly steadily increasing the gain until the first instability is observed. As a results in those cases the beam was oscillating at large amplitudes before from the beginning, a pattern not observed at higher feedback gains with fresh beams (Fig. 6). The spoiled emittance might have severely affected the growth rate and thus these data points could not be trusted. For several data points second measurements with fresh beam were performed – in that case those measurements were taken. All the unreliable data for which no measurement with fresh beam was available was discarded. In order to avoid this if the measurements are repeated in the future we propose performing the calibration starting with a large feedback gain and gradually lowering it, reinjecting fresh beams after each observed instability.

After filtering the data the resulting dependence of the instability growth rate on the feedback gain was found to be linear, as expected (see Fig. 7). Also, the growth rate slope reduces gradually with the phase, as expected. The magnitude of the slope yields the calibration factor for the feedback gain (i.e. a setting of g units drives an instability with an exponential rise time of t turns) for any following measurements.

At the time of experiment no on-the-fly analysis of the tune shift was done, as it was complicated by the presence of tune significant tune jitter of the order of 1×10^{-4}. Nevertheless, the tune shift sign was verified using a bunch-by-bunch tune monitor (the base-band Q-meter, BBQ). Post-factum, an accurate reconstruction of the tune turned out to be possible only for the measurements at 45 deg phase, where the tune shift are large enough to overcome the noise while the instability growth rate is still slow enough to obtain sufficient data points during the developing instability. The tune was computed using a moving window of 1024 turns with a Fast Fourier Transform (FFT) with zero-padding and a Hanning filter – a standard technique for identifying the major tune lines in spectra of realistic accelerator data [15]. An example of the observed tune shift can be seen in the center panel of Fig. 5. As the anti-damper is turned on and the instability starts developing, the tune changes from its average unperturbed value (blue line) to the shifted one (red line). Periodic 'bumps' can also be seen in the data which are attributable to the tune feedback system.

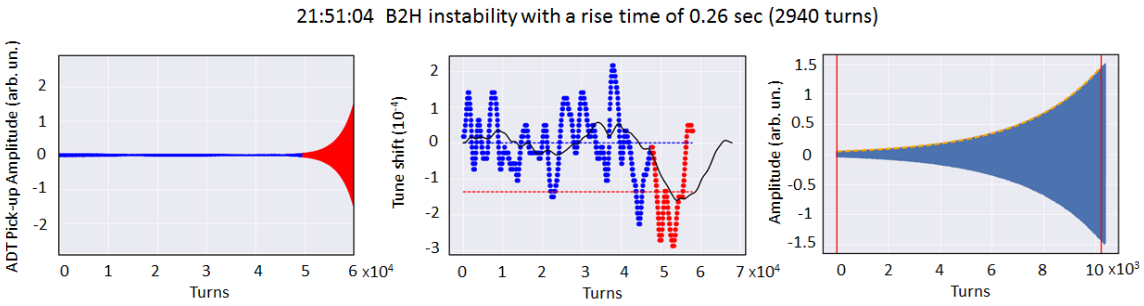

Figure 5: An example of an instability observed during the feedback calibration process. Left – the full 64'000 turn acquisition of the center of mass position, the unstable area is highlighted in red. Right – zoom-in of the instability. The dashed yellow line represents an exponential fit of the data. Center – the frequency domain: the black line shows the moving average of the tune. The blue and red lines indicate mean values for the stable and unstable regions.

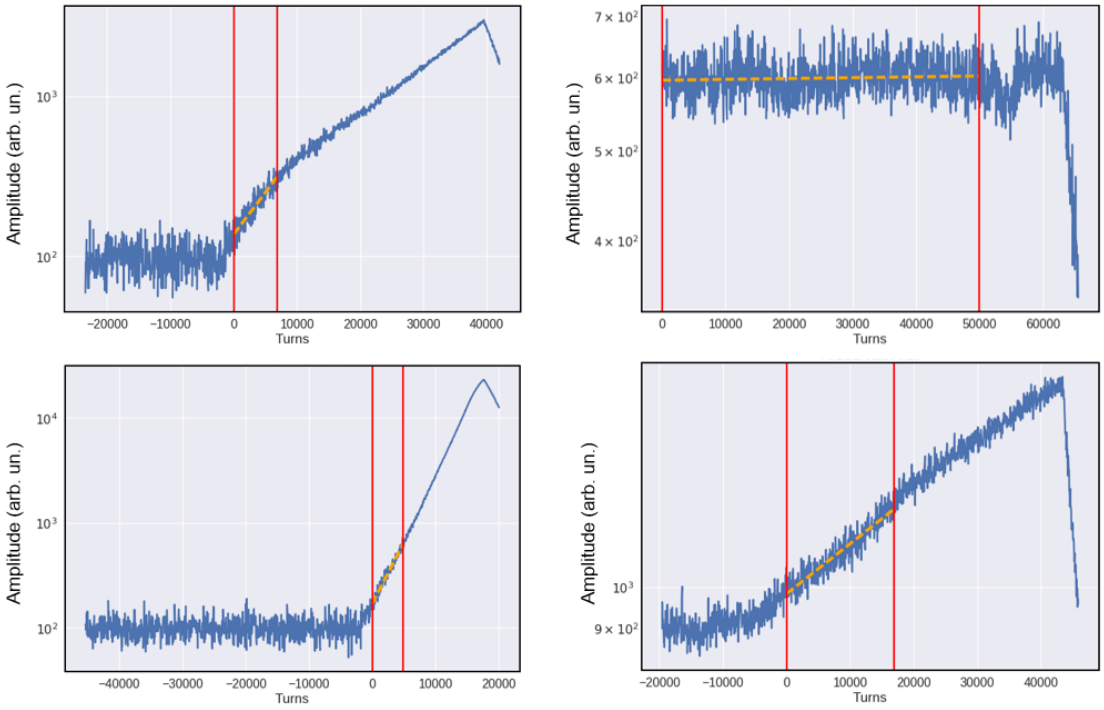

Figure 6: Left – examples of 'good' data: center of mass position oscillations start at around 100 units and increase exponentially as the destabilising feedback is turned on. The growth rate is determined as the maximum slope (dashed orange line) observed at the onset of the instability (highlighted with two vertical red lines). Turn 0 corresponds to the start of the process. Right – examples of 'bad' data, with the beams likely having suffered an instability before, which had affected the bunch distribution: the initial center of mass position oscillates around larger values, as the feedback gains is increased no growth is observed in some cases. Even though in some cases an exponential growth is observed, the slope might be affected by the blown up emittance.

The tune is observed to vary linearly with the feedback gain, and its slope matches what the growth rate measurement implies: 1.3×10^{-2} vs. $\frac{1}{2\pi} 6.39 \times 10^{-2} = 1.1 \times 10^{-2}$ (Fig. 7). A small discrepancy of about 15% can be explained by the uncertainty of the tune shift determination procedure. An uncertainty in damper phase can also contribute to the discrepancy, while it is expected to remain rather small at the above-mentioned less than 1 deg level.

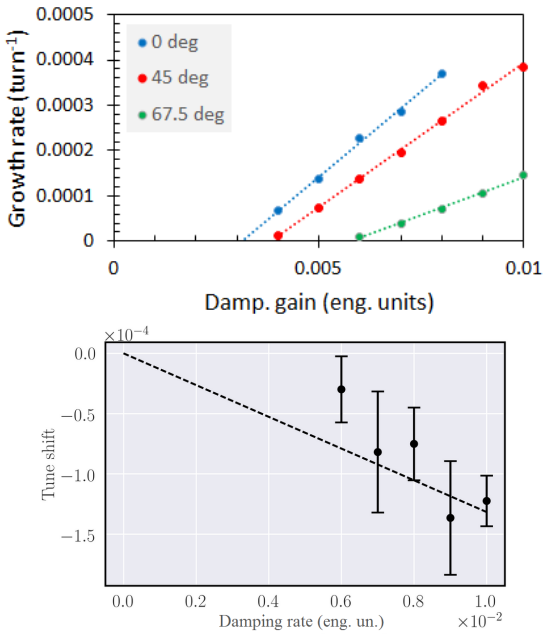

Figure 7: The transverse feedback drives an instability (top) and induces a tune shift proportional to its gain (bottom).

Stability Diagram scans

After calibrating the feedback we performed a series of measurements at different octupole settings. At each setting the feedback gain was gradually increased in small steps until reaching the limit of stability. At this point the feedback phase was increased – as the SD contour should have an increasing distance to the origin at increasing phase, the beam should return to stable conditions at higher phases. This procedure has been repeated for a few different phases between 0 and 90 deg. At each step the feedback gain was kept constant for about 30 sec, which should have excluded potential impact of latency effects. This time window has been chosen following a recent study, where latency effects could be excluded in single bunch octupole threshold measurements with sufficiently short 1 min steps [16]. In our experiment, an instability was declared as soon as the beam centroid excursion from the reference orbit exceeded 200 μm – a value comparable to the rms transverse size of the beam. In this case the feedback was automatically switched back to a resistive stabilizing mode with a strong damping time of 200 turns (Fig. 8). We used an automated script to perform these stability diagram scan. The procedure of locating the the boundary of stability typically took 5 min or less per data point (octupole current, feedback phase setting). The

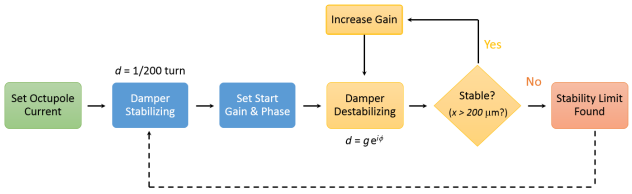

Figure 8: Procedure for measuring SDs: feedback gain is increased at a fixed phase until a threshold amplitude is exceeded, then the feedback is reverted back to the stabilizing mode.

measurement was only performed in one of the LHC beams – Beam 2 and only in the horizontal plane due to resource and machine constraints at the time of the study.

The beam emittance should remain unaffected throughout the measurement – a condition which was closely monitored during the experiment by means of the beam synchrotron radiation monitor. Therefore, in order to save time, the beam was only re-injected when an emittance growth by more than 10% had been observed. A disadvantage of this approach is that the distribution tails might have been affected by previous measurements, as they correspond to a large tune shift and thus play a crucial role in Landau damping. While no systematic study of the effect was attempted during this proof-of-principle test, several data points were measured twice to check reproducibility of the results. The results with an 'old' and with a 'fresh' beam turned out to be in good agreement within 10% and less fluctuation.

RESULTS AND DISCUSSION

Landau damping by LHC octupoles

The shape of the measured SDs at 11, 17, and -11 A qualitatively matches the expectations from simple linear SD theory. Both the height and the width scale with the octupole current: e.g. the SD for 17 A turns out to be around 50% taller than the SD for 11 A, which matches the 1.5 times higher current (Fig. 9). The second measurement for 11 A current made at a lower chromaticity of 3 units matches within 10 – 20 percent the first one performed at 14 units. The negative octupole polarity offers around 30% greater coverage of the negative tune shifts. This illustrates the reason why negative octupole polarity is preferred, namely to suppress impedance-driven instabilities in LHC that feature negative mode frequency shifts. The exact figure of the required threshold gain will eventually depend on the details of the beam distribution.

Injection-to-injection spread of the strength of Landau damping, measured over 5 consecutive injections at 11 A and 0 deg phase (i.e. resistive anti-damper) turned out to be rather small at around 7% indicating sufficient reproducibility of the beam distribution. The 7% value gives a lower limit on the systematic uncertainty for all subsequent measurements.

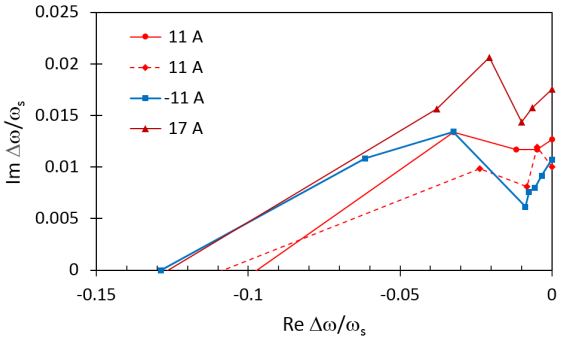

Figure 9: The measured height of the diagrams scales linearly with the octupole current with the negative octupole polarity providing around 30% larger coverage of negative mode frequency shifts, which are relevant for coherent beam stability. LHC SDs were measured at 450 GeV in the horizontal plane, solid lines – $Q' = 14$, dashed line – $Q' = 3$. Real and imaginary tune shifts are normalized by the synchrotron frequency.

Depending on the damper phase and thus the direction of the tune shift, the modes would probe different parts of the octupole SD: for the imaginary shift it would be the center that is nearly independent of the beam distribution or the octupole polarity, whereas for the real shift it would be the tail of the diagram that strongly depends on the beam parameters (i.e. emittance, intensity, bunch profile, etc.), which all vary slightly from fill to fill. Hence, measurements probing the central SD peak around 0 deg damper phase are less affected by these beam parameter variations, while the SD tails (probed around ±90 deg damper phase) underlie a significant uncertainty.

Quantitatively, from simple detuning considerations one would expect to measure about a factor two larger SDs than what was observed in the experiment. There are several factors that could contribute to this discrepancy. First of all, it has to be mentioned that the mode complex frequency shift is affected by the machine's impedance and neglecting the latter might lead to a considerable miscomputation of the octupole threshold as demonstrated in Fig. 10. If one excites with a resistive feedback, the border of the SD is crossed at a different location, closer to the tail of the diagram, at a factor two lower feedback gain. If one then uses this lower gain to infer the octupole threshold without considering the mode shift produced by the impedance, one might underestimate the threshold by about a factor two.

Other effects include natural machine nonlinearities that might generate a linear detuning with amplitude equivalent to about −2.5 A of octupole current [17–19] and linear coupling that can distort the amplitude detuning from the Landau octupoles, reducing the footprint locally, but leading as well to a large second order amplitude detuning [18, 20]. While the coupling had been corrected to a sufficiently low value in the beginning of the test at $|C^-| = 0.001$, it may have drifted away from this initial value over time, which would shrink the octupole tune footprint and result in a slightly smaller the SD for larger $|C^-|$ values [21].

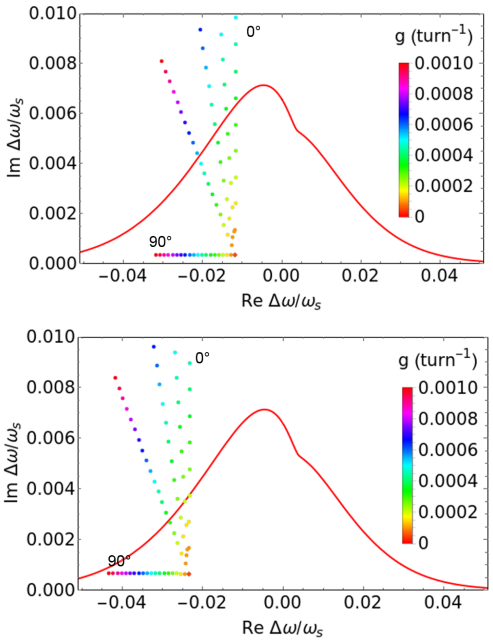

Figure 10: Machine impedance creates a negative tune shift, affecting the position of SD crossing when a destabilizing feedback is applied. Top – nominal machine impedance; bottom – double machine impedance. The SD depicted by a red line corresponds to a Gaussian beam with 1 μm rms normalized emittance and 2.5 A positive octupole current. Various feedback gains for 5 equidistant phases between 0 and 90 deg are shown as coloured dots.

Finally, although space charge on its own does not provide Landau damping for the rigid dipole mode, as pointed out by Möhl [22], it does modify the SD produced by lattice nonlinearities. In general, an interplay of octupole detuning and nonlinear space charge may be important as observed in particle tracking simulations [23]. When the strength of space charge detuning is small relative to other sources its impact can be estimated analytically in a simple model [24], assuming a quasi-parabolic transverse distribution [25], coasting beam conditions, and a linear space charge detuning (the model can be extended to bunched beams [26], although the impact of the bunching is minor). Depending on the strength of space charge, it leads to a negative real tune shift of the SD maximum, a widening of the diagram, and a slight reduction of its height. For the studied parameters, the impact of space charge should be relatively weak providing a shift of the SD of around $\Delta_0 = 10^{-4}$. Nevertheless, the space charge interaction could significantly affect the spread of betatron frequencies and thus the Landau damping when the machine nonlinearities were small enough, i.e. during the feedback calibration, as discussed below.

Comparison with macro-particle simulations

To investigate the space charge issue further we performed macro-particle simulations in the PyHEADTAIL macroparticle tracking code, which performs 6-dimensional tracking [27–29]. The tracking utilizes smooth optics approximation and a drift/kick model for non-linear synchrotron motion, treating the accelerator ring as a collection of interaction points connected by ring segments where the beam is transversely transported via transfer matrices. Nonlinear optics effects such as chromatic detuning and octupolar amplitude detuning are applied as effective tune shifts for each individual macro-particle. Collective effects, arising from impedance, space charge, or external feedback are applied at the interaction points where the beam is longitudinally divided into a set of slices via a 1D particle-in-cell (PIC) algorithm.

The natural machine nonlinearities were modelled by a -2.5 A equivalent octupole linear amplitude detuning ($\sim 10^{-5}$ rms tune spread). The numerical model also included nonlinear longitudinal motion inside the RF bucket while linear coupling effects were neglected, since they are expected to have little effect on beam stability if the coupling is sufficiently well corrected as discussed before. Without space charge, 1×10^6 macro-particles have been tracked for 1×10^6 turns. Simulations including self-consistent space charge (via a 2.5D slice-by-slice PIC algorithm) are based on 3×10^6 macro-particles being tracked during 60×10^3 turns corresponding to a machine time of more than 5 s.

Tracking results shown in Fig. 11 demonstrate that SC significantly affects the instability growth rate for a given gain of the destabilizing feedback increasing the stable area. With SC included the simulation results remain in good agreement with the experimental observations. This highlights the importance of including the space charge interaction into the picture when comparing experimental data to models or tracking results. Further comprehensive numerical studies including all potential effects are required to understand the magnitude and shape of the measured SDs and compare with the available analytical models.

Table 2: Key simulation parameters in addition to Table 1

Parameter	Value
Chromaticity	$Q'_{x,y} = 15$
Transverse tunes	$(Q_x, Q_y) = (64.28, 59.31)$
Synchrotron tune	$Q_s = 4.9 \times 10^{-3}$

CONCLUSION

In this proof-of-principle test we have demonstrated that the active feedback system can be used as a source of controlled impedance to probe the strength of Landau damping. The experiment has been carried out in the LHC at the injection energy of 450 GeV using single bunches at low intensity. First, the active feedback system has been calibrated in order to produce arbitrary complex tune shifts. Both tune shift and instability growth rate have been demonstrated to increase linearly with the feedback gain, as expected. Then, the feedback has been utilized to directly measure the strength of Landau damping by gradually increasing its gain until a transverse activity is observed. The possibility of exploring the SD by changing the damper phase has also been demonstrated. The results are in qualitative agreement with the details of theoretical SD predictions. A more extensive quantitative analysis (in particular comparing to tracking simulations with space charge) is required to include effects of lattice nonlinearities and coherent effects in the picture.

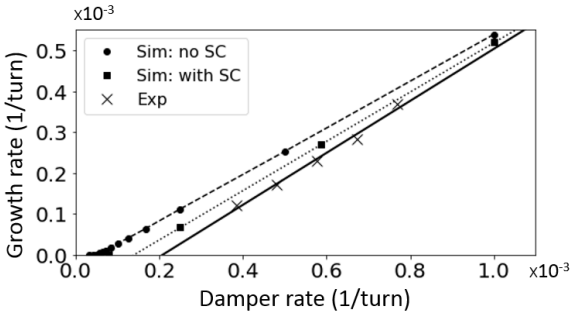

Figure 11: Instability growth rate scales linearly with the damper gain, allowing to calibrate the feedback strength. The non-zero gain required to start an instability is caused by natural nonlinearities of the machine. Overall, experimental data (crosses and the solid line) are in good agreement with numerical simulations (squares and the dotted line). Numerical simulations performed with space charge show a greater amount of feedback gain required to destabilize the beam than in the no-space-charge case (circles and the dashed line), emphasizing the importance of accounting for the space charge interaction at the LHC injection energy, $E = 450$ GeV.

The technique has a potential to become a fast non-destructive tool for measuring the strength of Landau damping throughout the accelerator cycle. In LHC it would be well suited for studies at the top energy, where the constraints arising from Landau damping are the tightest and the effect of space charge is negligible. In order to explore this potential, further studies including the top energy (6.5 TeV at the moment, with plans to reach the nominal 7 TeV in the future) should be carried out after the current Long Shutdown. This approach also has a potential of shedding light on the interplay between Landau damping and space charge – an area where currently one has to rely on computationally demanding macroparticle simulations. For example, at LHC after demonstrating sufficient safety for the machine, the bunch intensity could be increased up to $\sim 10^{11}$ p or $\Delta Q_{SC} \sim Q_s$ at 450 GeV. This would allow investigating how an increasing space charge force affects Landau damping by the octupoles.

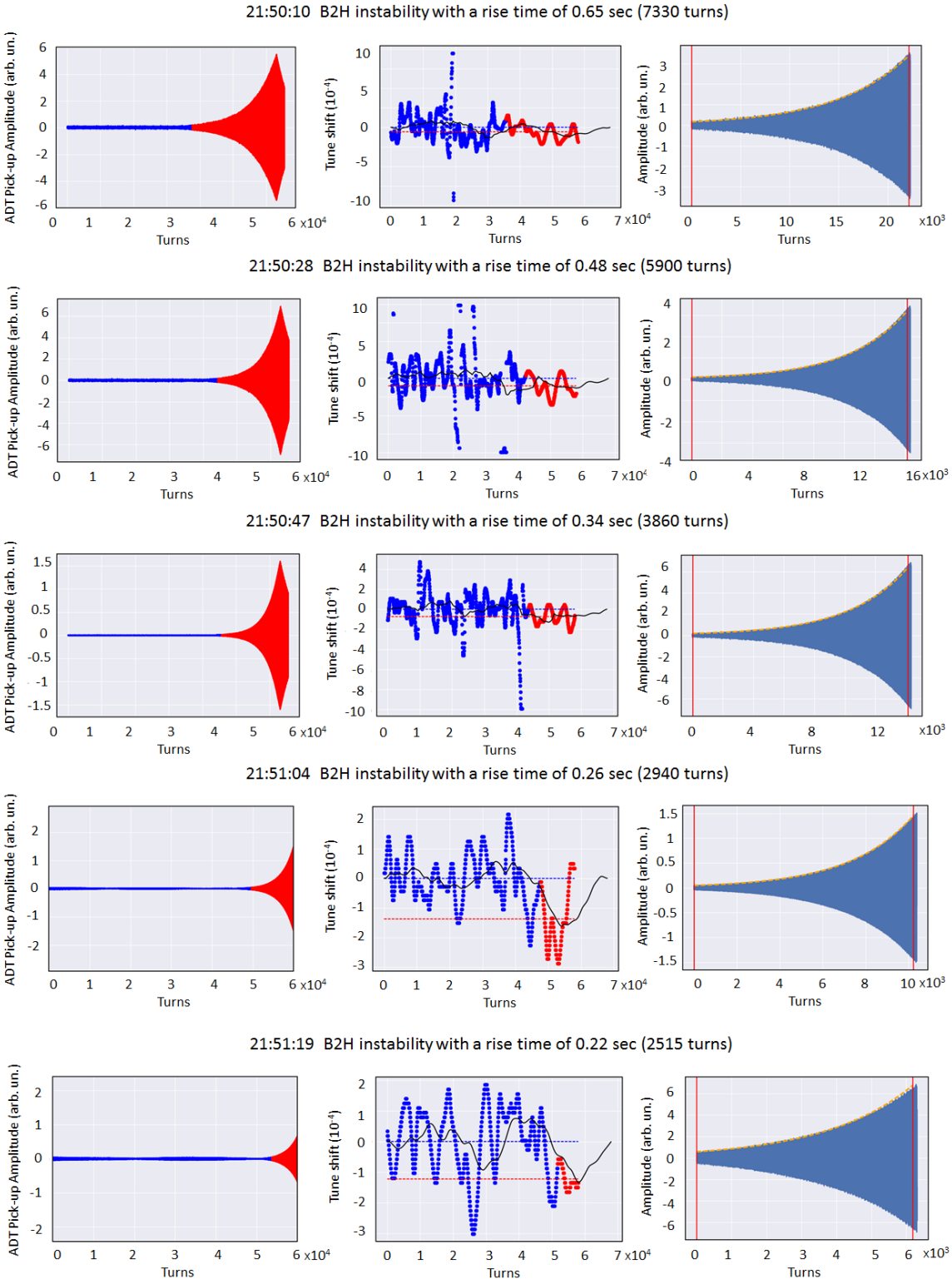

Figure 12: Beam position data for a 45 degree phase. Left – oscillation envelope over 64000 acquisition turns, the unstable area, defined by a crossing of the threshold, is shown in red. Center – tune variation over time, obtained with a moving FFT window of 2000 turns; solid black line shows the moving average, dashed blue – average stable tune, dashed red - average unstable tune. Right – exponential amplitude blow-up observed in the unstable region; exponential fits are shown in orange.

ACKNOWLEDGEMENTS

The authors would like to thank Alexey Burov (FNAL) for sharing his ideas on the use of a transverse feedback as a source of controlled impedance which triggered this research. We express our gratitude to the LHC Operations Team and especially Francesco Velotti for a fruitful and productive collaboration that helped sketching a realistic plan and ultimately successfully carry out tests. We shall also thank Lukas Malina for his insightful tips on the analysis of turn-by-turn data, Gianluigi Arduini for his comments on the paper, and Ewen Maclean and Tobias Persson for discussion on the sources of lattice nonlinearities in LHC.

REFERENCES

[1] A. W. Chao and M. Tigner, "Handbook of accelerator physics and engineering," Singapore: World Scientific (2006)

[2] K. Hübner, A. G. Ruggiero, and V. G. Vaccaro, "Stability of the coherent transverse motion of a coasting beam for realistic distribution functions and any given coupling with its environment," CERN-ISR-TH-RF-69-23

[3] V. Kornilov, O. Boine-Frankenheim, W. Kaufmann, and P. Moritz, "Measurements and Analysis of the Transverse Beam Transfer Function (BTF) at the SIS 18 Synchrotron," GSI-Acc-Note-2006-12-001, GSI, Darmstadt (2006)

[4] Y. Luo, W. Fischer, A. Marusic and M. Minty, "Measurement and Simulation of Betatron Coupling Beam Transfer Function in RHIC," doi:10.18429/JACoW-IPAC2018-MOPMF010

[5] C. Tambasco *et al.*, "First BTF Measurements at the Large Hadron Collider," doi:10.18429/JACoW-IPAC2016-WEPOY030

[6] C. Tambasco *et al.*, "Beam Transfer Function and Stability Diagram," these proceedings

[7] T. Pieloni *et al.*, "MD 3292: Summary of BTF studies MD Block 3&4," CERN, 4 Dec 2018 `https://indico.cern.ch/event/776844`

[8] A. W. Chao, "Physics of collective beam instabilities in high-energy accelerators," New York, USA: Wiley (1993) 371 p

[9] A. Burov, "Nested Head-Tail Vlasov Solver," Phys. Rev. ST Accel. Beams **17**, 021007 (2014) doi:10.1103/PhysRevSTAB.17.021007

[10] S. Antipov *et al.*, "IOTA (Integrable Optics Test Accelerator): Facility and Experimental Beam Physics Program," JINST **12**, no. 03, T03002 (2017) doi:10.1088/1748-0221/12/03/T03002

[11] E. Stern, J. Amundson, and A. Macridin, "Suppression of Instabilities Generated by an Anti-Damper with a Nonlinear Magnetic Element in IOTA," doi:10.18429/JACoW-IPAC2018-THPAF068

[12] A. Butterworth *et al.*, "LHC transverse feedback," in Proc. 6th Evian Workshop on LHC beam operation, Evian Les Bains, France, Dec 2015

[13] W. Höfle *et al.*, "Transverse feedback in the HL-LHC era," 5th Joint HighLumi LHC - LARP Meeting Fermilab, USA, Oct 2015

[14] O. S. Brüning, P. Collier, P. Lebrun, S. Myers, R. Ostojic, J. Poole and P. Proudlock, (Eds.), "LHC Design Report Vol.1: The LHC Main Ring," doi:10.5170/CERN-2004-003-V-1

[15] R. Bartolini, A. Bazzani, M. Giovannozzi, W. Scandale, and E. Todesco, "Tune evaluation in simulations and experiments," Part. Accel. **52**, 147-177 (1996) CERN-SL-95-84-AP.

[16] X. Buffat *et al.*, "Summary of instability observations at LHC and implications for HL-LHC," CERN, 9 Jul 2019, `https://indico.cern.ch/event/831847/`

[17] M. McAteer *et al.*, "Magnet polarity checks in the LHC," CERN-ACC-NOTE-2014-0012

[18] E. H. Maclean, R. Tomás, F. Schmidt, and T. H. B. Persson, "Measurement of nonlinear observables in the Large Hadron Collider using kicked beams," Phys. Rev. ST Accel. Beams **17**, no. 8, 081002 (2014). doi:10.1103/PhysRevSTAB.17.081002

[19] E. H. Maclean, "Observations relating to MCDO alignment," CERN, Geneva, Switzerland, Feb 2019 `https://indico.cern.ch/event/812944/`

[20] E. H. Maclean, F. Carlier, M. Giovannozzi, T. Persson, and R. Tomás, "Effect of Linear Coupling on Nonlinear Observables at the LHC," doi:10.18429/JACoW-IPAC2017-WEPIK092

[21] L. R. Carver, X. Buffat, K. Li, E. Métral, and M. Schenk, "Transverse beam instabilities in the presence of linear coupling in the Large Hadron Collider," Phys. Rev. Accel. Beams **21**, no. 4, 044401 (2018). doi:10.1103/PhysRevAccelBeams.21.044401

[22] D. Möhl, "On Landau damping of dipole modes by nonlinear space charge and octupoles," Part. Accel. **50**, 177 (1995).

[23] V. Kornilov, O. Boine-Frankenheim, and I. Hofmann, "Stability of transverse dipole modes in coasting ion beams with nonlinear space charge, octupoles, and chromaticity," Phys. Rev. ST Accel. Beams **11**, 014201 (2008). doi:10.1103/PhysRevSTAB.11.014201

[24] E. Métral and F. Ruggiero, "Stability diagrams for Landau damping with two-dimensional betatron tune spread from both octupoles and non-linear space charge," CERN-AB-2004-025-ABP.

[25] E. Métral and A. Verdier, "Stability diagram for Landau damping with a beam collimated at an arbitrary number of sigmas," CERN-AB-2004-019-ABP.

[26] K. Y. Ng, "Landau damping of space-charge dominated Fermilab Booster beam," FERMILAB-CONF-08-410-AD.

[27] K. Li *et al.*, "Code development for collective effects," doi:10.18429/JACoW-HB2016-WEAM3X01

[28] E. Métral *et al.*, "Beam Instabilities in Hadron Synchrotrons," IEEE Trans. Nucl. Sci. **63**, no. 2, 1001 (2016). doi:10.1109/TNS.2015.2513752

[29] A. Oeftiger, "An Overview of PyHEADTAIL," CERN-ACC-NOTE-2019-0013

[30] E. H. Maclean *et al.*, "Tune-footprint through the LHC cycle," CERN, 17 Oct 2017, `https://indico.cern.ch/event/672805/`

APPENDIX

An example of gathered data for the 45 deg phase, obtained during feedback calibration when increasing the gain from 0.006 to 0.010 units (Fig. 12). Turn-by-turn data was gathered for 64000 turns for each event.